Current Indian Science

Content list available at: https://benthamscience.com/journal/213

RESEARCH ARTICLE

Pharmacological Evaluation of Phyto-Phospholipid Complexes (Phytosome) for Diabetic Neuropathy and Nephropathy Regulating Oxidative Stress and Inflammatory Mediators in Streptozotocin-Induced Diabetic Rats

Shivam[1,2,*] and Asheesh Kumar Gupta[2]

[1]*Department of Pharmacy, R. V. Institute of Pharmacy, Bijnor Moradabad Road, State Highway No. 76, Uttar Pradesh (NCR), 246728, Moradabad, India*

[2]*School of Pharmaceutical Sciences, Faculty of Pharmacy, IFTM University, Delhi Road, NH-24 Moradabad, Lodhipur Rajput, Uttar Pradesh 244102, India*

Abstract:

Introduction:

Diabetes mellitus is characterized by chronic hyperglycemia leading to complications such as neuropathy and nephropathy. Oxidative stress and inflammation are key contributors to its pathogenesis. In this study, a novel therapeutic strategy utilizing phyto-phospholipid complexes (phytosomes) was developed to enhance the bioavailability and efficacy of plant bioactives in mitigating these diabetic complications.

Objective:

To evaluate the anti-diabetic, neuroprotective, and nephroprotective effects of phyto-phospholipid complexes (phytosomes) and assess their impact on oxidative stress and inflammatory mediators as potential mechanisms for anti-diabetic effects.

Methods:

Acute oral toxicity was evaluated using a fixed-dose method as per OECD guidelines. We administered a single oral dose of the phyto-phospholipid complex (PPC) formulation at 250 mg/kg body weight to the experimental rats, and the animals were monitored for signs of toxicity for a period of 14 days. The animals were divided into different groups: control, diabetic (induced by streptozotocin [STZ]), and treatment groups (CME and PPC formulations). Diabetes was induced in experimental rats using a single parenteral dose of STZ (60 mg/kg) intraperitoneally. Treatment groups received PPC (250 mg/kg) or CME (250 mg/kg) daily for a specified duration. The sciatic nerve and kidney tissues from all groups of rats were isolated at the end of the experiment for histopathological evaluation. Tissues were processed, sectioned, and stained to examine structural changes under a light microscope.

Results and Discussion:

The phytosomal formulation demonstrated potent effects in mitigating streptozotocin (STZ)-induced diabetes complications, with improvements in both nephroprotective and neuroprotective effects compared to the combined methanolic extract (CME) of all plants. The PPC (polyherbal phytosomal formulation) at a dosage of 250 mg/kg, alongside STZ (60 mg/kg), showed statistically significant (p <0.05) improvements in comparison to CME (250 mg/kg) and was comparable to glibenclamide (0.25 mg/kg). Histopathological analysis confirmed that PPC treatment significantly reduced damage to the kidneys and sciatic nerve.

Conclusion:

The use of novel phytosomal delivery systems for herbal medicines enhances the bioavailability of polar extracts, thus improving therapeutic outcomes and patient compliance. Treatment with PPC reduced the risk of diabetic complications, likely due to enhanced kidney function and modulation of inflammatory mediators.

Keywords: Diabetic neuropathy, Diabetic nephropathy, Oxidative stress, Streptozotocin, Phytosomes, Inflammatory mediators.

Article History	Received: May 13, 2025	Revised: August 04, 2025	Accepted: August 18, 2025

1. INTRODUCTION

Diabetes is a chronic condition that causes an increase in glucose levels in blood plasma, leading to serious problems such as nerve-related problems like diabetic neuropathy (nerve damage) and renal problems like diabetic nephropathy (kidney damage) [1]. These complications are common in people with uncontrolled diabetes and can greatly affect their quality of life. Diabetic neuropathy can cause symptoms such as pain, tingling, and numbness, while diabetic nephropathy often leads

to kidney failure if left untreated [2]. The current treatments for these complications often come with side effects, and there is a growing need for safer, more effective alternatives. Herbal medicine has gained attention because it tends to have fewer side effects and can target multiple aspects of the disease [3]. One promising approach is the use of phyto-phospholipid complexes, also known as phytosomes. Phytosomes are a type of drug delivery system that combines plant extracts with phospholipids, helping to increase the absorption and effectiveness of these compounds in the body. This technology improves the bioavailability of herbal treatments, making them more potent and easier for the body to absorb [4].

This research focuses on preparing phytosomes from various plant extracts that have been traditionally used to treat diabetes-related complications. The goal is to evaluate how these phytosomes can help manage diabetic neuropathy and nephropathy by regulating oxidative stress (damage caused by harmful molecules) and inflammatory mediators (substances that promote inflammation) [5]. Diabetic kidney disease, or diabetic nephropathy, is a microvascular complication of diabetes mellitus that leads to end-stage renal damage [6]. Diabetic glomerular lesions, decreased glomerular filtration rate, and variable urine albumin excretion are characteristics of diabetic nephropathy. The existence of inflammation in diabetic nephropathy has been previously verified by several experimental and clinical studies [7].

This study introduces a novel approach by combining bioactive-rich plant extracts with nanocarrier-based phytosomes to enhance therapeutic efficacy in diabetes-associated complications. Many plant extracts have been studied for their potential to prevent or mitigate complications associated with diabetes mellitus (DM). Polyherbal formulations are preferable to individual formulations [8]. We used a rat model in which diabetes is induced by streptozotocin (STZ), a chemical that raises blood sugar levels, to mimic the conditions seen in humans with diabetes. The study aims to assess the safety, effectiveness, and potential therapeutic benefits of these phytosomal formulations in treating diabetes-related nerve and kidney damage. By investigating how these phytosomes work, this research hopes to provide new insights into safer, plant-based treatments for managing the complications of diabetes, particularly focusing on reducing inflammation and oxidative stress, which are key drivers of tissue damage in diabetic neuropathy and nephropathy [9]. The medicinal plants Chirata, fenugreek, and sesame selected for this formulation are safe and non-toxic in animal studies [10].

2. MATERIAL AND METHODS

2.1. Chemicals and Reagents

Streptozotocin procured from Sigma Aldrich, glibenclamide procured from Aurobindo Pharma, and other chemicals procured from SD Fine chemicals. Analytical-grade reagents and compounds were used for all other compounds in this study.

* Address correspondence to this author at the Department of Pharmacy, R. V. Institute of Pharmacy, Bijnor Moradabad Road, State Highway No. 76, Uttar Pradesh (NCR), 246728, India and School of Pharmaceutical Sciences, Faculty of Pharmacy, IFTM University, Delhi Road, NH-24 Moradabad, Lodhipur Rajput, Uttar Pradesh 244102, India; E-mail: shivamdmohit@gmail.com

2.2. Collection and Authentication of Drugs

The study utilized a combination of freshly harvested plants and herbs purchased from a local market at an Ayurvedic store in Majholi Khas, Bilari, Uttar Pradesh, India. The authenticity of the plants was verified by the Botanical Institute Raw Material and Herbarium Museum, Delhi (RHMD), thereby ensuring the credibility of the botanical materials used. The specific plants and their reference numbers are as follows. The reference numbers are NISCAIR/ RHMD/Collected/2021/4165-42-1 for *Swertiachirayitaleaves,* NISCAIR/RHMD/Collected/2021/4165-42-2 for seeds of*Trigonellafoenum-graecum*, and NISCAIR/RHMD/ Collected/2021/4165-42-3 for seeds of *Sesamum indicum*.

2.3. Extraction of Material

Dried powdered plant material from leaves of *Swertiachirayita,* seeds of the *Trigonella* methi, and seeds of the *Sesamum indicum* (500 g) was extracted using traditional extraction methods in a Soxhlet apparatus on a heating mantle. First, petroleum ether was used to remove fatty materials, such as lipids, and then three liters of methanol were added at a temperature not to exceed 45ºC, each time until the extraction was finished. A sealed container was used to condense the methanolic extract of all three herbs over rota vapors under low pressure [11]. The methanolic extracts of these plants contain active phytochemicals, such as flavonoids and phenolics; therefore, we selected the methanolic extract.

2.4. Preparation of Phyto-Phospholipid Complexes(phytosomes)

The different phytosome complexes extract of combined methanolic extracts (Ratio 1:1:1) of leaves of *Swertiachirayita,* seeds of the*Trigonellafoenumgraecum*and seeds of the *Sesamum indicum* were prepared by the solvent evaporation method. Phytosomes were prepared using the solvent evaporation technique by incorporating a combined methanolic extract of *Swertiachirayita, Trigonella foenum-graecum,* and *Sesamum indicum*. Precise amounts of soya lecithin, cholesterol, and the combined herbal extracts were dissolved in a mixture of methanol and transferred to a dry, round-bottom flask. The organic solvent mixture was evaporated at 60 rpm and 40°C for 15 minutes in a rotary evaporator under low pressure to obtain a thin lipid film coated on the inner wall of the flask. The lipid film was hydrated with phosphate buffer of pH 7.4 while stirring at 60 rpm for 1 hour at room temperature. The preparation was then subjected to ultrasonic probe sonication for 30 minutes to produce small vesicles and was stored at 4°C for further examination. The obtained phospholipid–extract complex was dried and kept in a sealed desiccator at 2–8°C for further use [12, 13].

Particle size and zeta potential were measured using dynamic light scattering (DLS). EE% was determined *via* ultracentrifugation [14].

2.5. Acute Toxicity Studies

An oral acute toxicity study of the plant extract was performed in accordance with OECD Guideline No. 423, as recommended by the Organization for Economic Co-operation and Development. In this study, we administered different

doses of 5, 50, 300, and 2000 mg/kg body weight to experimental rats. This investigation utilized healthy rats that were neither pregnant nor nulliparous. Rats were individually monitored. The rats were observed for 48 hours to detect any behavioral or neurological changes, including tremors, convulsions, salivation, diarrhoea, sleepiness, lacrimation, and alterations in feeding behavior, which could indicate signs of acute toxicity in rats treated with the extract. The combined extracts of both drugs were administered orally to overnight-fasted rats according to the guidelines. Observation was continued for an additional 14 days to monitor for any delayed signs of toxicity [15].

2.6. Experimental Animals and Research Protocol

For research methodologies and the use of animals in experiments, albino rats (body weight 200–250 g, age 8–12 weeks) were procured from the School of Pharmaceutical Sciences, Department of Pharmacy at IFTM University's animal house. In this study, a total of 33 animals were used: 3 non-pregnant, nulliparous rats for acute oral toxicity, and 30 rats (both male and female) for the pharmacological study. During the 28-day study, animals were maintained under carefully controlled conditions to ensure their well-being and the reliability of the experimental results. Relative humidity was maintained between 45% and 55%, and the temperature was maintained at 25±2°C. Water and food pellets were provided ad libitum.

The project was approved by the Institutional Animal Ethics Committee (IAEC) of the School of Pharmaceutical Sciences, IFTM University. It was registered under registration number 837/PO/ReBiT/S/04/CPCSEA and conducted following the guidelines set forth by the Committee for the Purpose of Control and Supervision of Experiments on Animals (CPCSEA), India. The animals were sacrificed by cervical dislocation after the testing phases. A midline incision was made to open the anterior abdominal wall, followed by careful dissection of the kidneys. Next, an incision was made in the thigh area near the hind limb to dissect and remove the thick, whitish, stick-like structure known as the sciatic nerve [16, 17].

2.7. Induction of Experimental Diabetes

Diabetes, diabetic neuropathy, and nephropathy were induced in the experimental animals using streptozotocin (STZ). For diabetes induction, freshly prepared STZ (60 mg/kg) in 0.1 M citrate buffer solution with pH 4.5 was injected intraperitoneally into the experimental rats. A 20% glucose solution was provided to the STZ-treated rats to prevent hypoglycaemic mortality. Blood glucose levels in the STZ-treated rats were measured after **72 hours.** Rats with fasting blood glucose levels of 250 mg/dL or above were considered diabetic [10].

2.8. Experimental Design

The experimental animals were divided into five groups, and each group contained six animals.

Experimental Group I: Normal control (distilled water orally 2ml/ kg)

Experimental Group II: Diabetic control (STZ 60 mg/kg body weight)

Experimental Group III: Standard anti-diabetic drug (Glibenclamide dose 0.25 mg/kg)

Experimental Group IV: Combined methanolic extract (CME) of all plants (250 mg/kg)

Experimental Group V: Phyto-Phospholipid Complexes (PPC) (250 mg/kg)

2.9. Fasting Blood Glucose

Blood glucose levels of the rats were determined by collecting a tail blood sample. Following the trial, information on body weight, food intake, and water consumption was also recorded and analyzed. A more accurate evaluation of baseline glucose regulation was possible because the fasting period, typically 12 to 16 hours, ensured that the blood glucose levels measured represented fasting glucose levels [18].

2.10. Behavioural Parameters

Evaluation and recording of the formulation's impact on body weight (BW), food intake (FI), water intake (WI), and urine elimination during 14 days [19].

2.11. Assessment of Mechanical Allodynia

To assess mechanical allodynia in streptozotocin-induced diabetic rats, place the rat on a wire mesh platform. Mechanical allodynia was assessed using a von Frey filament applied to the hind paw. The withdrawal response was recorded, with increased sensitivity or withdrawal at lower force indicating the presence of allodynia. Tests were repeated to ensure consistency and accuracy of the measurements [20].

2.12. Biochemical Parameters

By day 28, at the end of an 18-hour fasting period, blood was collected retro-orbitally under light anesthesia. The animals were euthanized by cervical dislocation after blood collection. The blood was transferred into dry, clean test tubes and allowed to clot for 30 minutes at room temperature [21]. Serum was then separated from the clot by centrifugation at 3000 rpm for 10 minutes. This serum was used for the estimation of glucose, total cholesterol, triglycerides, LDL, VLDL, and HDL [22]. The liver was carefully excised, washed thoroughly with an adequate amount of saline, dried, and weighed. It was then homogenized in phosphate buffer, and total glycogen was estimated from the liver homogenate [23, 24].

2.13. Oxidative Stress

The collected samples (the left side sciatic nerves) were meticulously cleaned of blood before being promptly frozen and maintained in a freezer set at -80°C for analyses of tissue malondialdehyde (MDA), glutathione (GSH), catalase (CAT), and superoxide dismutase (SOD) levels [25, 26].

2.14. Serum and Urine Renal Function Parameters

The level of serum creatinine was determined using a commercially available diagnostic kit supplied by Erba

Chem-7. Each rat was placed in a metabolic cage for individual urine collection over a 24-hour period. Urine volume was recorded using a measuring cylinder, with units expressed as mL/24 h [27]. The urine samples were analyzed for creatinine (Jaffe method), urea (urease L-glutamate dehydrogenase), and urinary proteins (biuret method) using Erba Chem-7 kits. Urinary type IV collagen was also determined using ELISA kits supplied by Abcam (ab6586). The 24-hour urinary albumin excretion rate (UAER) was calculated following protocols established in previous research [28, 29].

2.15. Estimation of Inflammatory Cytokines

Serum levels of IL-6, TGF-β1, and TNF-α were measured using ELISA kits. Blood was collected through cardiac puncture, allowed to clot, and then centrifuged at 3000 × g for 10 minutes to obtain the serum at 4°C. Serum samples were kept at -80°C until analysis. Specific monoclonal antibodies were pre-coated onto a 96-well ELISA plate. Standard solutions and diluted serum samples were added to wells and incubated at 37°C for 1–2 hours. After washing with PBST, a biotin-labeled secondary antibody was added, followed by incubation. After washing, streptavidin-HRP was added with another incubation period, followed by a washing step. To develop color, TMB substrate was added; color developed for 15–30 minutes, after which the reaction was stopped by adding 2N sulfuric acid. Absorbance at 450 nm was measured, and cytokine concentration was calculated from the standard curve. Results were expressed in pg/mL or ng/mL, representing inflammation with diabetic conditions [30, 31].

2.16. Estimation of PMP22 and MPZ Expression by Western Blot and qPCR

The levels of Peripheral Myelin Protein 22 (PMP22) and Myelin Protein Zero (MPZ) were examined by Western blot and quantitative PCR (qPCR). Sciatic nerve tissues or cultured Schwann cells were harvested and homogenized in ice-cold lysis buffer with protease inhibitors. The mixture was centrifuged at 12,000 × g for 15 minutes at 4°C, and the supernatant was used for further experiments.

For Western blotting, the protein concentration was initially determined by BCA. Equal quantities of protein were resolved on SDS-PAGE and blotted onto a PVDF membrane. The membrane was blocked with 5% BSA and left overnight at 4°C with primary antibodies against PMP22 or MPZ. After washing, HRP-linked secondary antibodies were added, and the protein bands were detected with an ECL detection system. To conduct gene expression analysis, TRIzol reagent was used to extract total RNA, which was subsequently reverse-transcribed to generate cDNA. Specific primers for MPZ and PMP22 were subsequently used for qPCR, with GAPDH or β-actin as the housekeeping gene for normalization [32, 33].

2.17. Examination of the Sciatic Nerve: Histopathology

The sciatic nerve was carefully removed from the experimental animals, rinsed with saline, and fixed in 10% formalin for 24–48 hours. After fixation, the tissue was dehydrated stepwise using increasing concentrations of ethanol (70%, 80%, 95%, and 100%), followed by clearing in xylene. The tissue was then embedded in paraffin wax. Thin sections, approximately 4–6 µm thick, were cut using a microtome and mounted on clean glass slides. The slides were deparaffinized with xylene, rehydrated through decreasing concentrations of ethanol, and stained with Hematoxylin and Eosin (H&E) to visualize tissue structure. After staining, the sections were again dehydrated, cleared in xylene, and covered with a coverslip. The stained slides were examined under a light microscope to assess structural damage associated with diabetic neuropathy [34, 35].

2.18. Histopathology of the Kidney

Kidneys were harvested from the experimental animals, washed with saline to remove blood, and fixed in 10% formalin for 24–48 hours. Following fixation, the tissues were gradually dehydrated using increasing concentrations of ethanol (70%, 80%, 95%, and 100%), cleared in xylene, and embedded in paraffin wax. Thin sections, approximately 4–6 µm thick, were cut using a microtome and mounted onto glass slides. The sections were deparaffinized with xylene, rehydrated through descending concentrations of ethanol, and stained with Hematoxylin and Eosin (H&E) to visualize kidney structure. After staining, the slides were dehydrated, cleared in xylene, and covered with coverslips. The prepared slides were examined under a light microscope to assess structural alterations and tissue damage associated with diabetic nephropathy [35, 36].

2.19. Statistical Analysis

Tukey's multiple comparison analysis is utilized as a post hoc test after one-way ANOVA to examine all the data, which are submitted as means with norm error means (±SEM). It was deemed statistically significant at $p < 0.05$. The statistical analysis was conducted using GraphPad Prism (version 5.0) software (GraphPad Software, Inc., La Jolla, California, United States).

3. RESULTS

3.1. Acute Toxicity Study

The combined methanolic extract of all plants was found to be practically non-toxic when administered orally to rats at doses of 5, 50, 300, or 2000 mg/kg. Therefore, it is proposed that the extracts of *Swertia chirayita*, *Trigonella foenum-graecum*, *Sesamum indicum*, and their combined extract (1:1:1) are safe for herbal use. The animals' responses were observed to be normal, supporting the safety of these herbs. Based on these findings, the dose of the combined extract was selected as 250 mg/kg body weight.

3.2. Anti-diabetic Study of Phyto-Phospholipid Complexes(phytosomes)

3.2.1. Glucose Level Estimation

Fasting blood glucose levels were measured across five groups on Days 7, 14, 21, and 28 to evaluate the anti-hyperglycemic effect of the treatment. The results showed significant differences among the groups for each day ($p < 0.001$). Post-hoc analyses using Tukey's HSD indicated that

Group II consistently had significantly higher glucose levels compared to Groups I, III, IV, and V at all time points ($p < 0.001$). Groups III, IV, and V showed significant reductions in glucose levels over time, suggesting improved glucose control compared to Group II. Statistical significance was denoted by 'a' (Group II significantly different from Group I) and '***' (significant differences compared to Group I) (Fig. **1**).

3.2.2. Body Weight (BW), H2O Intake (WI), food Intake (FI), and Urine Out (UO)

Body weight, food intake (FI), water intake (WI), and urine output (UO) among the groups ($p < 0.001$). Post-hoc Tukey's HSD tests showed that Group II had significantly higher FI, WI, and UO than Groups I, III, IV, and V ($p < 0.001$). Groups III, IV, and V had significantly different body weights and reduced FI, WI, and UO compared to Group I. Statistical significance: 'a' indicates Group II differs from Group I ($p < 0.05$); '*'** denotes significant differences from Group I ($p < 0.001$) (Table **1**).

3.2.3. Impact on Diabetic-Induced Mechanical Allodynia

Beginning on day 28 after STZ, when mechanical allodynia became apparent, diabetic rats were given oral treatment once daily for 7 days, either with a vehicle or a Polyherbal formulation. When diabetic rats were repeatedly treated with a combination of a methanolic extract and a polyherbal formulation, mechanical allodynia was greatly alleviated, whereas it persisted in diabetic rats treated with a vehicle.

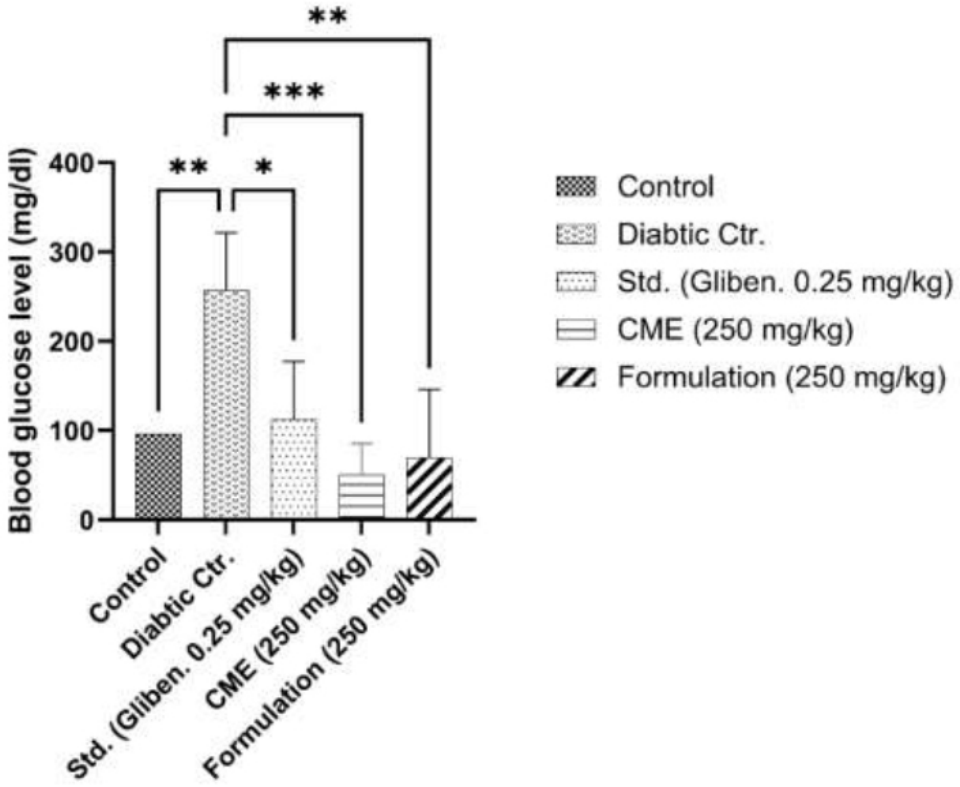

Fig. (1). Effect of herbal formulation on fasting blood sugar level.

Table 1. Effect on feed intake, water intake, urine output, and body weight.

Groups	Rat Body Weight (g)	Food Intake (g/day)	Water Intake (mL/day)	Urine Output (mL/day)
Group 1	170±4.25	26.65±5.45	48.33±8.62	7.55±3.35
Group 2	152.50±4.85a	45.67±4.56a	92.65±3.51a	36.38±4.65a
Group 3	171.50±6.15a***	42.25±5.35***	66.47±5.50***	16.34±3.62***
Group 4	185.00±7.3***	36.42±5.32***	55.55±7.52***	15.45±3.05***
Group 5	181.33±5.32a***	32.44±3.66***	53.35±8.45***	12.42±3.88***

Note: One-Way ANOVA showed significant differences in body weight, FI, WI, and UO among groups ($p < 0.001$). **Tukey's HSD** revealed Group II differed significantly from Groups I, III, IV, and V ($p < 0.001$). **'a'** denotes significant differences from Group I ($p < 0.05$); **'*'**** indicates significant differences from Group I ($p < 0.001$).

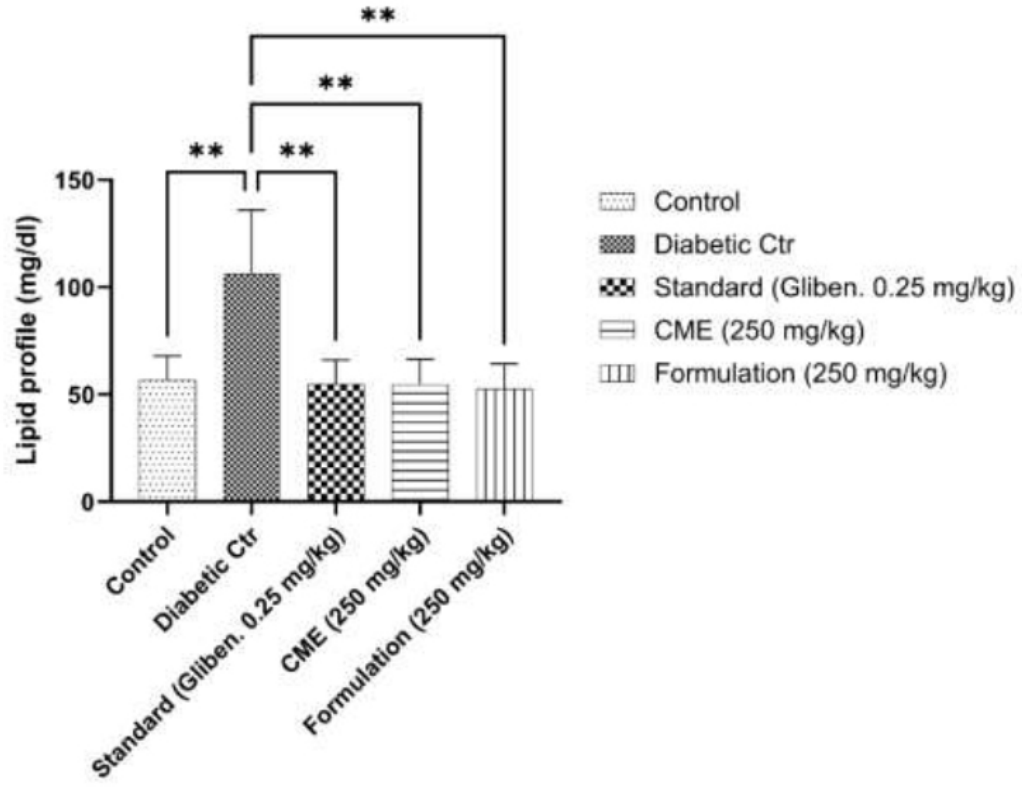

Fig. (2). Effect of phyto-phospholipid complexes on serum lipid profile.

3.2.4. Biochemical Parameters

Serum cholesterol, triglycerides, HDL, and LDL among groups showed that Group II had significantly higher triglycerides and LDL compared to Groups I, III, IV, and V. Groups III, IV, and V had significantly different cholesterol, triglycerides, HDL, and LDL compared to Group I. The prepared formulation showed protective effects on biochemical parameters (Fig. **2**).

3.2.5. Oxidative Stress

The antioxidant parameters were assessed across different treatment groups. In Group I, the baseline levels of glutathione (GSH), malondialdehyde (MDA), catalase (CAT), and superoxide dismutase (SOD) were measured. Group II showed a significant decrease in GSH and an increase in MDA, CAT, and SOD compared to Group I, indicating a possible imbalance in antioxidant defense. Group III demonstrated further reductions in GSH, along with higher MDA levels and decreased CAT and SOD activities, suggesting more severe oxidative stress. Group IV showed improvements in antioxidant levels, with GSH, MDA, CAT, and SOD approaching normal values. Finally, Group V also showed improved antioxidant enzyme activity, though not reaching the levels seen in Group I, suggesting some beneficial effects of the treatment. These results highlight varying levels of oxidative stress and the impact of the treatments on antioxidant defense mechanisms (Supplementary Table **1**).

3.2.6. Impact on Renal Function Tests

The various groups were assessed for different kidney function parameters. Group I served as the control, showing normal levels of urine volume, urinary urea, serum creatinine, urine creatinine, and protein in urine. In Group II, significant alterations were observed, with a marked decrease in urine volume and urinary urea, alongside increased serum creatinine and decreased urine creatinine. This suggested kidney dysfunction. Group III showed improvements, with increased urine volume, reduced serum creatinine, and better overall kidney function. Groups IV and V also demonstrated positive effects, with improvements in kidney function parameters compared to Group II, though not reaching the levels seen in the control group. Additionally, when assessing the urinary albumin excretion rate (UAER), advanced glycation end products (AGES), and type IV collagen excretion, Group II had significantly elevated values, indicating kidney damage. Groups III, IV, and V showed reduced excretion of these markers, reflecting a potential therapeutic effect. However, Group III showed the greatest improvement in these markers, suggesting the greatest treatment benefit (Supplementary Tables **2** and **3**).

3.2.7. Impact of on Inflammatory Mediators

The levels of key inflammatory markers, including IL-6, TGF-β1, and TNF-α, were measured across different groups. In Group I, the levels of these markers were within the normal range, indicating a stable inflammatory profile. However, in Group II, all three markers increased significantly, suggesting

heightened inflammation and a potential negative impact on the kidney and overall health. In Groups III, IV, and V, the levels of IL-6, TGF-β1, and TNF-α were notably reduced compared to Group II, reflecting the beneficial effects of the treatments. Group III showed the greatest reduction, suggesting the most effective therapeutic impact on inflammation, while Groups IV and V also showed improved inflammatory profiles (Supplementary Table **4**).

3.2.8. Histopathology of Kidneys

The kidney injury score was determined based on the extent of tubular degeneration, glomerular shrinkage, and urinary space enlargement observed in histopathological sections. Healthy Control Group (Fig. **3A**): Score 0 (Normal kidney structure with no pathological changes). STZ-Induced Diabetic Group (Fig. **3B**): Score 3–4 (Severe tubular degeneration, significant glomerular shrinkage, and increased urinary space). CME 250 mg/kg Treated Group (Fig. **3C**): Score 2–3 (Partial improvement in glomeruli but persistent tubular destruction). PPC 250 mg/kg Treated Group (Fig. **3D**): Score 1–2 (Mild tubular degeneration and reduced glomerular shrinkage). Glibenclamide 0.25 mg/kg Treated Group (Fig. **3E**): Score 1–2 (Similar to PPC, showing partial kidney protection). The results suggest that PPC and glibenclamide provided better renal protection compared to CME, reducing kidney injury severity.

Tubular Vacuolization (Yellow Arrow): Indicates cellular injury.

Tubular Atrophy (Blue Arrows): Shrinking of tubules due to chronic injury.

Interstitial Inflammation (Red Arrows): Presence of inflammatory cells, indicating tissue damage and immune response. Each field (A-E) can be given a score based on the percentage of affected tubules.

0 = No damage, 1 = <10% of tubules affected, 2 = 10-25% of tubules affected, 3 = 25-50% of tubules affected and 4 = >50% of tubules affected

Image A – No significant damage (Score 0)

Image B – Severe damage with atrophy, vacuolization, and inflammation (Score 3-4)

Images C, D, and E-Moderate tubular damage (Score 2-3) (Fig. **3**). The extent of tubular injury observed is shown in Table **2**.

3.2.9. Examination of Sciatic Nerve Histopathology

Histopathology of the sciatic nerve revealed normal nerve tissue with no inflammatory or degenerative alterations in the hematoxylin and eosin (H&E) sections of the control group treated with 0.5% CME, without diabetes induction. The typical configuration of nerve fibers with elongated Schwann cells, myelin sheaths, and longitudinally oriented nuclei was observed. The diabetic group treated with STZ exhibited nerve abnormalities, including axonal swelling. In contrast, in group IV (diabetic rats treated orally with mixed methanolic extract, 250 mg/kg BW), H&E sections displayed reduced axonal swelling and more uniformly distributed nerve fibers.

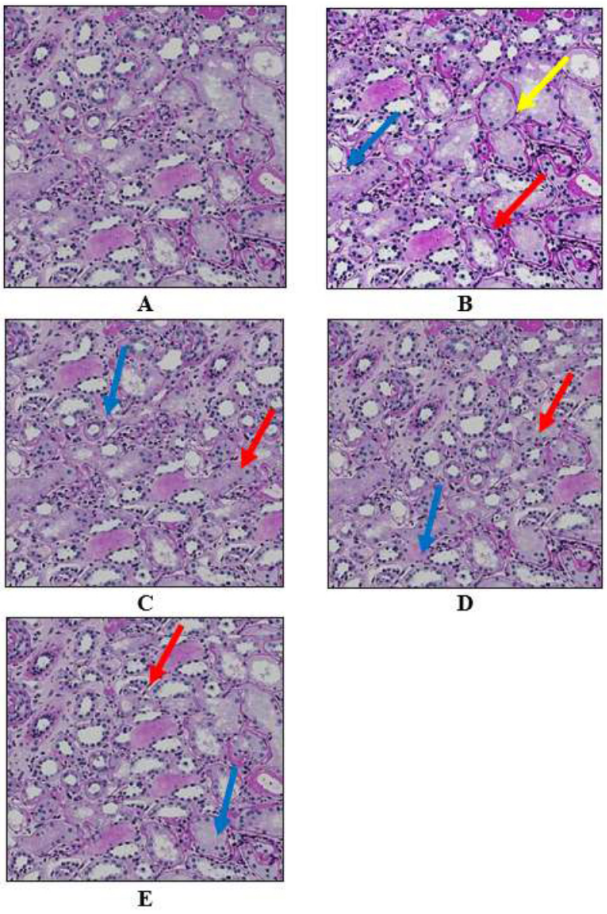

Fig. (3A-E). Histopathology of kidneys.
Tubular Vacuolization (Yellow arrow).
Tubular Atrophy (Blue arrow).
Interstitial Inflammation (Red arrow).
A: Normal control rats had normal histology of the kidneys (Score 0). **B:** Diabetic control animals showed severe damage with atrophy, vacuolization, and inflammation (Score 3-4). **C:** Rats administered a dose of 0.25 mg/kg of Glibenclamide showed moderate damage (Score 2-3). **D:** Rats which received 250 mg/kg of CME show improvement in inflammation and tissues damaged (Score 2-3). **E:** Rats treated with 250 mg/kg of PPC show minimal atrophy, vacuolization, and inflammation (Score 1-2).

When compared to the diabetic control group, diabetic rats treated with PPC (250 mg/kg) exhibited well-organized nerve fibers, elongated Schwann cells, and decreased axonal swelling (Fig. **4**). Examination of H&E-stained sciatic nerve sections revealed distinct differences among the experimental groups. The control group (A) showed a typical nerve fiber arrangement with elongated Schwann cells. The diabetic control group (B) exhibited pronounced axonal swelling. Treatment with glibenclamide at 0.25 mg/kg (C) still showed some axonal swelling. The CME-treated group at 250 mg/kg (D) displayed several cases of lipoid degeneration. Finally, the PPC-treated group at 250 mg/kg (E) showed evenly aligned nerve fibers with minimal structural damage.

Table 2. Tubular injury score based on the given histological images.

Image	Tubular Vacuolization (Yellow)	Tubular Atrophy (Blue)	Interstitial Inflammation (Red)	Estimated Tubular Injury Score
A	Not Present	Not Present	Not Present	0 (No injury)
B	Present	Present	Present	3-4 (Severe injury)
C	Not Present	Present	Present	2-3 (Moderate injury)
D	Not Present	Present	Present	2-3 (Moderate injury)
E	Not Present	Present	Present	1-2 (Minor injury)

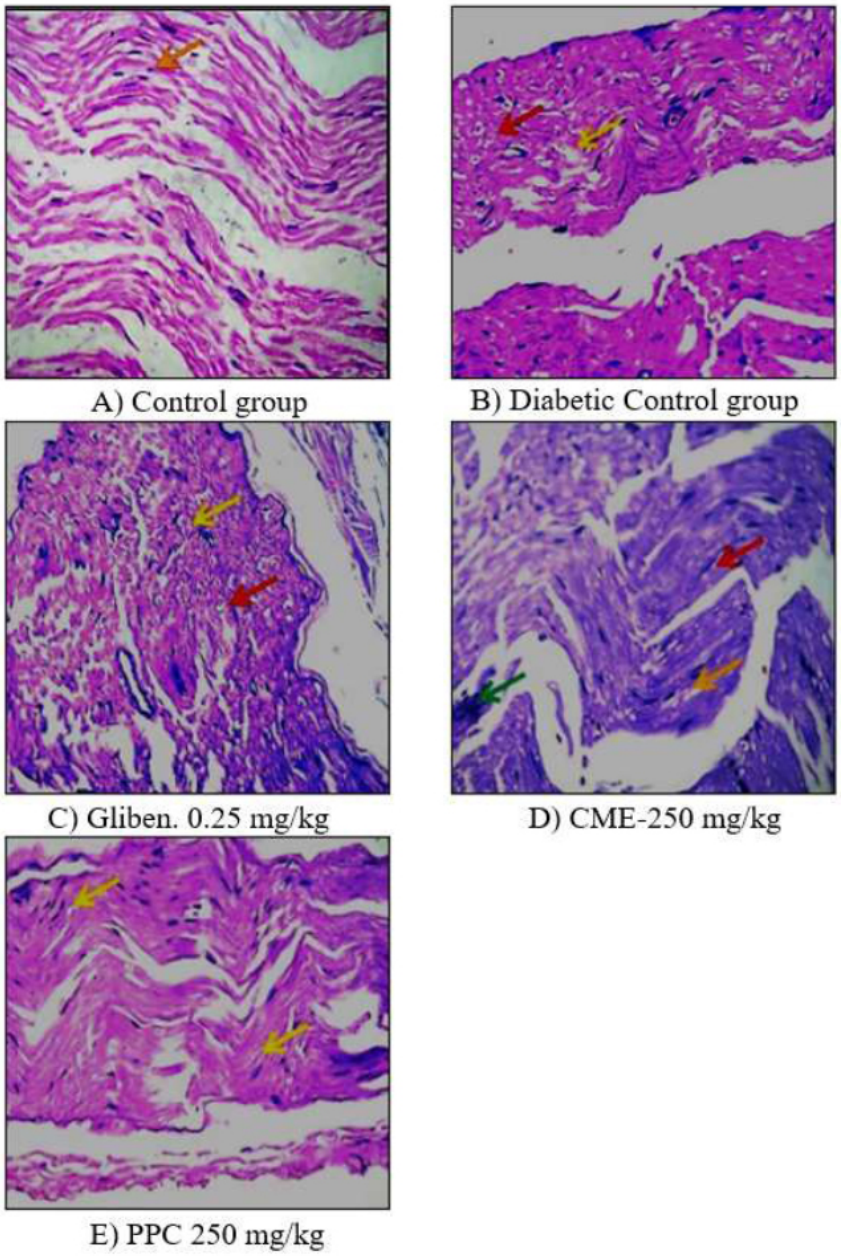

Fig. (4). Histopathology of sciatic nerve.
Scale bar = 200 µm, 10X magnification of camera.
A: Control animal not treated showed normal arrangement of nerve fibres with elongated Schwann cells. **B:** The diabetic control group presented axonal swelling and vacuolar degeneration. **C:** Animals treated with Glibenclamide 0.25 mg/kg exhibited axonal swelling of nerve fibres. **D:** The CME-250 treated group showed several lipid degenerations, and **E**, the PPC 250 mg/kg treated group presented uniformly arranged nerve fibres. Red arrow: Vocuolar degeneration, Yellow arrow: Schwann cell, Green arrows: Regeneration nerve fibres.

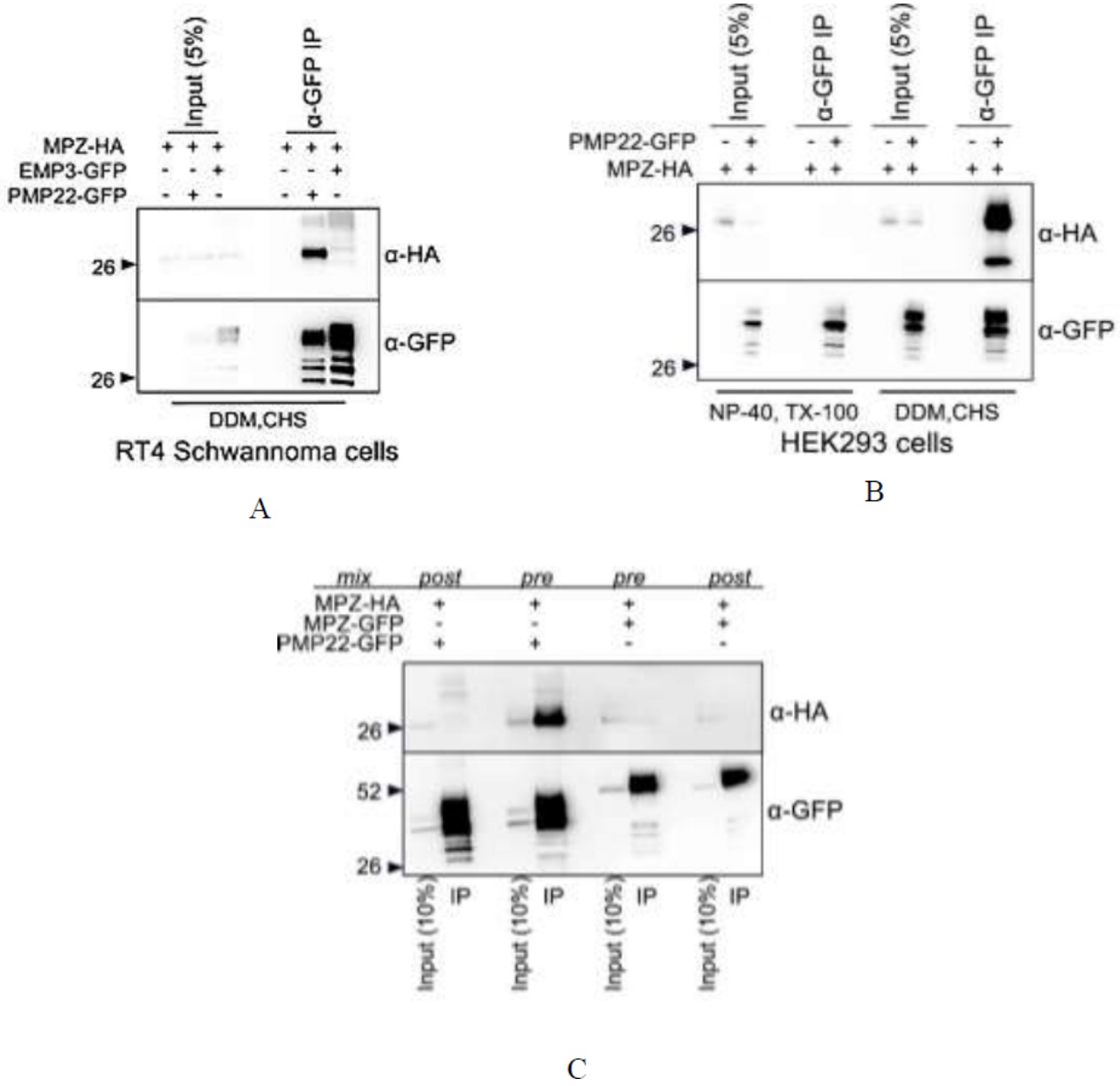

Fig. (5). MPZ interacts with PMP22 to form a protein complex in both HEK293 and RT4 Schwannoma cells.

3.2.10. Effect on PMP22, MPZ

Western blot analysis of PMP22 and MPZ showed a significant reduction in protein levels in the diabetic group compared with the control group, indicating myelin degeneration due to hyperglycemia. Treatment with the phyto-phospholipid complex (PPC) significantly restored PMP22 and MPZ levels, with effects comparable to those of the glibenclamide-treated group. qPCR analysis confirmed these findings, as PMP22 and MPZ mRNA expression levels were downregulated in the diabetic group but significantly upregulated in PPC-treated rats, suggesting a protective effect on myelin integrity.

Our research indicated that PMP22 possesses a specific and robust interaction with MPZ in HEK293 cells and rat RT4 Schwannoma cells. As shown in Figure **5**, GFP-tagged PMP22 was capable of pulling down HA-tagged C-terminal MPZ when both the proteins were co-expressed in HEK293 cells (Fig. **5A**) and RT4 Schwannoma cells (Fig. **5B**). Conversely, no interaction was seen between EMP3 and MPZ, a protein homolog of PMP22 (Fig. **5C**). Immunoprecipitation experiments were performed with Sepharose beads coupled with α-GFP nanobodies.

A) The left panel illustrates a co-immunoprecipitation experiment in which MPZ, tagged with a C-terminal HA epitope, and PMP22, tagged with a C-terminal GFP, are co-expressed. These proteins are then immunoprecipitated using Sepharose beads conjugated with α-GFP nanobodies. The right panel presents the co-immunoprecipitation results. Lysates

from HEK293 cells co-transfected with MPZ-HA and PMP22-GFP were prepared using two different detergent combinations: 0.5% NP-40 and 0.5% Triton X-100, or 1% DDM and 0.2% CHS. The bead-bound complexes were washed with PBS containing the respective detergents, then eluted with SDS sample buffer. A 5% portion of the input lysate was also analyzed alongside the precipitated complexes through SDS-PAGE and immunoblotting, using mouse α-HA antibodies to detect MPZ-HA and mouse α-GFP antibodies to assess the efficiency of PMP22-GFP immunoprecipitation.

B) The co-immunoprecipitation approach described in A was applied to HEK293 cells, where PMP22-GFP and MPZ-HA were either co-expressed prior to cell lysis (pre-lysis) or expressed separately in different populations and combined after lysis (post-lysis). The interaction between PMP22-GFP and MPZ-HA, or between MPZ-GFP and MPZ-HA, was assessed. Immunoprecipitates, along with 10% of the input sample, were analyzed by immunoblotting using an anti-HA antibody to detect MPZ-HA. The results show that MPZ-HA interacts with MPZ-GFP, although this interaction is significantly weaker than the interaction with PMP22-GFP. Furthermore, both types of interactions (MPZ□MPZ and MPZ□PMP22) were detectable only when the proteins were expressed in the same cells before detergent lysis.

C) Co-immunoprecipitation experiments were performed to examine the interaction between PMP22-GFP and MPZ-HA in lysates from RT4 Schwannoma cells transiently transfected with DDM/CHS detergents. The results showed that MPZ-HA was successfully co-precipitated with PMP22-GFP. However, no interaction was observed between MPZ-HA and EMP3-GFP, a protein related to PMP22.

3.2.11. Cell Culture and Transfection

RT4 Schwannoma and HEK293 cell lines were procured *via* the Cell Culture Facility at the School of Pharmaceutical Sciences, IFTM University, Moradabad, Uttar Pradesh, in 2022. Cell identity was confirmed, and the lines were maintained in accordance with institutional biosafety and ethical guidelines.

RT4 Schwannoma cells and HEK293 cells were cultured under routine cell culture conditions. RT4 cells were cultured in RPMI-1640, whereas HEK293 cells were cultured in DMEM. The media were supplemented with 10% fetal bovine serum (FBS) and antibiotics—penicillin (100 U/mL) and streptomycin (100 μg/mL). The cells were grown at 37°C under a humidified atmosphere of 5% CO_2. For transfection experiments, cells were seeded to achieve about 70–80% confluency. Transient transfection was performed using Lipofectamine 2000 according to the manufacturer's instructions. Plasmids carrying MPZ-HA, PMP22-GFP, and EMP3-GFP were transfected into the cells singly or in combinations, as needed for each experimental condition.

3.2.12. Lysis and Co-Immunoprecipitation (Co-IP) Protocol

After 24-48 hours of transfection, cells were lysed in either 0.5% NP-40 and 0.5% Triton X-100 or 1% DDM and 0.2% CHS in phosphate-buffered saline (PBS) supplemented with protease inhibitors (Roche). Lysates were cleared by centrifugation at 12,000 × g for 10 minutes at 4°C. Supernatants were incubated with Sepharose beads conjugated with α-GFP nanobodies for 4 hours at 4°C with constant rotation. After incubation, beads were washed three times with PBS containing the respective detergents. Bound complexes were eluted by boiling in SDS sample buffer for 5 minutes at 95°C.

3.2.13. SDS-PAGE and Immunoblotting

Eluted protein samples and a small portion (5–10%) of the total cell lysate were loaded onto a 10% SDS-PAGE gel to separate the proteins. Once separated, the proteins were transferred onto PVDF membranes. To block non-specific binding, the membranes were incubated in 5% non-fat dry milk prepared in TBST (Tris-buffered saline with 0.1% Tween-20) for 1 hour at room temperature. After blocking, the membranes were kept overnight at 4°C with specific primary antibodies for further detection.

4. DISCUSSION

Diabetic nephropathy, the most common complication of diabetes mellitus, affects 30%–40% of diabetics and often leads to end-stage renal failure. Nearly half of these patients require kidney transplants or dialysis, which reduces their quality of life and increases their financial burden. Current anti-diabetic drugs are less effective at delaying the onset of diabetic nephropathy. Although drugs targeting the renin-angiotensin-aldosterone system have received clinical approval, they have yet to demonstrate significant benefits. While the exact molecular mechanisms underlying diabetic nephropathy remain unclear, substantial research has identified hyperglycemia-induced advanced glycation end-products (AGEs) as critical mediators in activating oxidative stress, inflammation, and fibrosis in diabetic nephropathy [37].

The animal dose of the phytosome complex (PPC) was calculated based on body surface area to translate to a human equivalent dose (HED). According to the FDA's dose translation guidelines, the dose used in rats corresponds to an approximate human oral dose of 40.54 mg/kg. Previous clinical translation studies of similar phytosomes support the feasibility of our formulation in humans [38].

Histopathological changes are prominent indicators of renal injury. In diabetic nephropathy, these changes often manifest as enlarged glomeruli, tubular damage, and hemorrhagic lesions. Notably, PPC demonstrates remarkable efficacy in preserving renal structure. Our findings indicate that PPC exerts superior nephroprotective effects by interrupting the sequential cascade of oxidative stress, inflammatory signaling, and fibrosis associated with chronic diabetes. This enhanced protection is likely due to the diverse array of phytoconstituents present in PPC, each with recognized therapeutic properties. Thus, PPC may be considered a potential therapeutic option for diabetic nephropathy; however, further human studies are needed to confirm its clinical benefits [39].

Over a 12-week period, this study also demonstrated a strong association between diabetic neuropathy and the structural damage observed in diabetic rats [40]. Diabetes

induces overexpression of inflammatory markers, leading to cellular dysfunction and death. While treated groups displayed healthy tissues, the diabetic control group showed inflammation and infiltration in the sciatic nerve and liver. As shown in Table **2**, MDA levels significantly decreased in the PPC-treated group, indicating improved oxidative stress status. Similarly, downregulation of TNF-α and IL-6 supports the anti-inflammatory potential of the phytosomal formulation.

PPC enhances the bioavailability of flavonoids through phospholipid-mediated membrane permeability, surpassing conventional extracts in cellular uptake and therapeutic efficacy. Polyherbal formulations such as PPC demonstrate enhanced therapeutic effects compared to single-drug approaches due to synergistic activity, multi-target actions, and reduced side effects. Several studies have shown that combining bioactive compounds from different plant sources can improve pharmacokinetics and therapeutic outcomes in complex diseases like diabetes and neuropathy. Consistent with these findings, the PPC-treated group in our study exhibited superior improvements in both biochemical and histopathological parameters compared to groups treated with individual extracts.

CONCLUSION

The present study successfully developed and characterized a phyto-phospholipid complex (PPC) for enhanced delivery of plant bioactives. In streptozotocin-induced diabetic rats, PPC demonstrated significant improvements in oxidative stress parameters, inflammatory mediators, and histopathological features associated with neuropathy and nephropathy. These findings support the potential of phytosomal systems as a promising therapeutic strategy for managing diabetes-associated complications.

PPC, as a polyherbal phytochemical formulation, provides significant neuroprotective and nephroprotective effects by modulating the complex pathways of oxidative stress and inflammation that drive complications in chronic diabetes. By combining methanolic extracts from multiple herbal plants, this study demonstrates that PPC may prevent and ameliorate diabetic complications, including diabetic neuropathy and nephropathy. Its ability to target multiple underlying mechanisms—reducing oxidative damage, controlling inflammation, and preventing fibrosis—suggests a comprehensive therapeutic potential.

While these results are encouraging, further research, particularly clinical trials in human populations, is essential to fully assess the safety, efficacy, and long-term benefits of PPC. Translating the positive effects observed in animal models into human therapy will require rigorous investigation to determine optimal dosing, potential side effects, and broader applicability.

In conclusion, PPC represents a promising candidate for the management of diabetic neuropathy and nephropathy. Our findings highlight its potential as a multi-targeted therapeutic approach, offering hope for improved treatment of these challenging diabetic complications. However, additional human-centered studies are necessary to confirm its effectiveness and fully explore its clinical potential.

AUTHOR'S CONTRIBUTIONS

It is hereby acknowledged that all authors have accepted responsibility for the manuscript's content and consented to its submission. They have meticulously reviewed all results and unanimously approved the final version of the manuscript.

LIST OF ABBREVIATIONS

DM	=	Diabetes Mellitus
DN	=	Diabetic Neuropathy
DN	=	Diabetic Nephropathy
GBM	=	Glomerular Basement Membrane
PPC	=	Phytosomal Polyherbal Formulation
CME	=	Combined Methanolic Extract
CPCSEA	=	Committee for Control And Supervision on Experimental Animals
STZ	=	Streptozotocin
GLC	=	Glibenclamide
VLDL	=	Very Low Density Lipoprotein
MDA	=	Malondialdehyde
CAT	=	Catalase
SOD	=	Superoxide Dismutase
TNF-A	=	Tumor Necrosis Factor-Alpha
IL-6	=	Interleukin-6
TGF	=	Transforming Growth Factor
ANOVA	=	Analysis of Variance

ETHICS APPROVAL AND CONSENT TO PARTICIPATE

The study was conducted after obtaining ethical committee clearance from the Institutional Animal Ethics Committee of the School of Pharmaceutical Sciences, IFTM University, under registration no. 837/PO/ReBit/S/04/CPCSEA and resolution no. IAEC/2022/2/03.

HUMAN AND ANIMAL RIGHTS

This study adheres to internationally accepted standards for animal research and follows the 3Rs principle. The ARRIVE guidelines were employed for reporting experiments involving live animals, promoting ethical research practices.

Animal experimentation was conducted in accordance with the rules and guidelines of the Committee for the Purpose of Control and Supervision of Experiments on Animals (CPCSEA), India.

CONSENT FOR PUBLICATION

Not applicable

AVAILABILITY OF DATA AND MATERIALS

All the data and supporting information are provided within the article.

FUNDING

None.

CONFLICT OF INTEREST

The authors declare no conflict of interest, financial or otherwise.

ACKNOWLEDGEMENTS

The authors would like to thank Dr. Sushil Kumar, Director, School of Pharmaceutical Sciences, IFTM University. We would like to thank the hospital staff in Moradabad for their cooperation during the study. We also extend our sincere gratitude to everyone involved, including the Chancellor (M. P. Pandey) and the Dean, Faculty of Pharmacy (Prof. Dr. Navneet Verma) of IFTM University, who greatly appreciated their full cooperation during the study. Finally, our gratitude extends to the Department of Pharmacy for its valuable contributions.

SUPPLEMENTARY MATERIAL

Supplementary material is available on the Publisher's website.

REFERENCES

[1] Li, S.; Wang, J.; Zhang, B.; Li, X.; Liu, Y. Diabetes Mellitus and cause-specific mortality: A population-based study. *Diabetes Metab J,* **2019**, *43*(3), 319-341. [http://dx.doi.org/10.4093/dmj.2018.0060] [PMID: 31210036]

[2] Kebede, S.A.; Tusa, B.S.; Weldesenbet, A.B.; Tessema, Z.T.; Ayele, T.A. Incidence of diabetic nephropathy and its predictors among type 2 Diabetes Mellitus patients at University of Gondar Comprehensive Specialized Hospital, Northwest Ethiopia. *J Nutr Metab,* **2021**, *2021*, 1-7. [http://dx.doi.org/10.1155/2021/6757916] [PMID: 34497725]

[3] Tsalamandris, S.; Antonopoulos, A.S.; Oikonomou, E.; Papamikroulis, G.A.; Vogiatzi, G.; Papaioannou, S.; Deftereos, S.; Tousoulis, D. The role of inflammation in diabetes: Current concepts and future perspectives. *Eur Cardiol,* **2019**, *14*(1), 50-59. [http://dx.doi.org/10.15420/ecr.2018.33.1] [PMID: 31131037]

[4] Chawla, R.; Chawla, A.; Jaggi, S. Microvasular and macrovascular complications in diabetes mellitus: Distinct or continuum? *Indian J Endocrinol Metab,* **2016**, *20*(4), 546-551. [http://dx.doi.org/10.4103/2230-8210.183480] [PMID: 27366724]

[5] Pop-Busui, R.; Ang, L.; Holmes, C.; Gallagher, K.; Feldman, E.L. Inflammation as a therapeutic target for diabetic neuropathies. *Curr Diab Rep,* **2016**, *16*(3), 29. [http://dx.doi.org/10.1007/s11892-016-0727-5] [PMID: 26897744]

[6] Zoja, C.; Xinaris, C.; Macconi, D. Diabetic Nephropathy: Novel molecular mechanisms and therapeutic targets. *Front Pharmacol,* **2020**, *11*, 586892. [http://dx.doi.org/10.3389/fphar.2020.586892] [PMID: 33519447]

[7] Donate-Correa, J.; Ferri, C.M.; Sánchez-Quintana, F.; Pérez-Castro, A.; González-Luis, A.; Martín-Núñez, E.; Mora-Fernández, C.; Navarro-González, J.F. Inflammatory cytokines in diabetic kidney disease: Pathophysiologic and therapeutic implications. *Front Med,* **2021**, *7*, 628289. [http://dx.doi.org/10.3389/fmed.2020.628289] [PMID: 33553221]

[8] Prajapati, D.P.; Patel, M.; Dharamsi, A. Beneficial effect of polyherbal formulation in letrozole induced Polycystic ovarian syndrome (PCOS). *J Tradit Complement Med,* **2022**, *12*(6), 575-583. [http://dx.doi.org/10.1016/j.jtcme.2022.08.003] [PMID: 36325242]

[9] Shriram, R.G.; Moin, A.; Alotaibi, H.F.; Khafagy, E.S.; Al Saqr, A.; Abu Lila, A.S.; Charyulu, R.N. Phytosomes as a plausible nano-delivery system for enhanced oral bioavailability and improved hepatoprotective activity of silymarin. *Pharmaceuticals,* **2022**, *15*(7), 790. [http://dx.doi.org/10.3390/ph15070790] [PMID: 35890088]

[10] Shivam, G.; Gupta, A.K. Toxicological assessment and anti-diabetic effects of combined extract of chirata, fenugreek and sesame on regulating TNF-α, TGF-β and oxidative stress in streptozotocin induced diabetic rats. *Curr Drug Discov Technol,* **2024**, *21*(1), e201023222477. [http://dx.doi.org/10.2174/0115701638252203230919092315] [PMID: 37870057]

[11] Mandal, V.; Mohan, Y.; Hemalatha, S.J.P.r. Microwave assisted extraction—an innovative and promising extraction tool for medicinal plant research. *Pharmacogn Rev,* **2007**, *1*(1), 7-18.

[12] Hashemi Gahruie, H.; Eskandari, M.H.; Sadeghi, R.; Hosseini, S.M.H.J.F. Atmospheric pressure cold plasma modification of basil seed gum for fabrication of edible film incorporated with nanophytosomes of vitamin D3 and tannic acid. *Foods,* **2023**, *12*(1), 71. [http://dx.doi.org/10.3390/foods12010071]

[13] Lu, M.; Qiu, Q.; Luo, X.; Liu, X.; Sun, J.; Wang, C.; Lin, X.; Deng, Y.; Song, Y. Phyto-phospholipid complexes (phytosomes): A novel strategy to improve the bioavailability of active constituents. *Asian J Pharm Sci,* **2019**, *14*(3), 265-274. [http://dx.doi.org/10.1016/j.ajps.2018.05.011] [PMID: 32104457]

[14] Hebballi, A.P.; Pujar, B.; Honnalli, S.S.; Hiremath, S.I.; Menasinkai, A.; Bakale, A.; Nadaf, S.; M.V., A.; Vadavalli, S. Establishment and validation of a robust reversed-phase HPLC method for the determination of Calotropis gigantea in bulk material and marketed product. *Curr Pharm Anal,* **2024**, *20*(8), 920-931. [http://dx.doi.org/10.2174/0115734129343858241007073450]

[15] Walum, E. Acute oral toxicity. *Environ Health Perspect,* **1998**, *106*(Suppl 2), 497-503. [http://dx.doi.org/10.1289/ehp.98106497] [PMID: 9599698]

[16] Nasiry, D.; khalatbary, A.R.; Ahmadvand, H.; Talebpour Amiri, F.; Akbari, E. Protective effects of methanolic extract of *Juglans regia* L. leaf on streptozotocin-induced diabetic peripheral neuropathy in rats. *BMC Complement Altern Med,* **2017**, *17*(1), 476. [http://dx.doi.org/10.1186/s12906-017-1983-x] [PMID: 28969623]

[17] Rashedy, A.H.; Solimany, A.A.; Ismail, A.K.; Wahdan, M.H.; Saban, K.A. Histopathological and functional effects of antimony on the renal cortex of growing albino rat. *Int J Clin Exp Pathol,* **2013**, *6*(8), 1467-1480. [PMID: 23923065]

[18] Koneri, R.; Samaddar, S.; Simi, S.M.; Rao, S. Neuroprotective effect of a triterpenoid saponin isolated from Momordica cymbalaria Fenzl in diabetic peripheral neuropathy. *Indian J Pharmacol,* **2014**, *46*(1), 76-81. [http://dx.doi.org/10.4103/0253-7613.125179] [PMID: 24550589]

[19] Saleem, U.; Amin, S.; Ahmad, B.; Azeem, H.; Anwar, F.; Mary, S. Acute oral toxicity evaluation of aqueous ethanolic extract of *Saccharum munja* Roxb. roots in albino mice as per OECD 425 TG. *Toxicol Rep,* **2017**, *4*, 580-585. [http://dx.doi.org/10.1016/j.toxrep.2017.10.005] [PMID: 29152463]

[20] Qureshi, Z.; Ali, M.N.; Khalid, M. An insight into potential pharmacotherapeutic agents for painful diabetic neuropathy. *J Diabetes Res,* **2022**, *2022*, 1-19. [http://dx.doi.org/10.1155/2022/9989272] [PMID: 35127954]

[21] Zaitsev, S.Y.; Belous, A.A.; Voronina, O.A.; Rykov, R.A.; Bogolyubova, N.V. Correlations between antioxidant and biochemical parameters of blood serum of duroc breed pigs. *Animals,* **2021**, *11*(8), 2400. [http://dx.doi.org/10.3390/ani11082400] [PMID: 34438857]

[22] Zhukov, I.S.; Ptukha, M.A.; Zolotoverkhaja, E.A.; Sinitca, E.L.; Tissen, I.Y.; Karpova, I.V.; Volnova, A.B.; Gainetdinov, R.R. Evaluation of approach to a conspecific and blood biochemical parameters in TAAR1 knockout mice. *Brain Sci,* **2022**, *12*(5), 614. [http://dx.doi.org/10.3390/brainsci12050614] [PMID: 35625001]

[23] Gejl, K.D.; Ørtenblad, N.; Andersson, E.; Plomgaard, P.; Holmberg, H.C.; Nielsen, J. Local depletion of glycogen with supramaximal exercise in human skeletal muscle fibres. *J Physiol,* **2017**, *595*(9), 2809-2821. [http://dx.doi.org/10.1113/JP273109] [PMID: 27689320]

[24] Díaz Martínez, A.E.; Alcaide Martín, M.J.; González-Gross, M. Basal values of biochemical and hematological parameters in elite athletes. *Int J Environ Res Public Health,* **2022**, *19*(5), 3059. [http://dx.doi.org/10.3390/ijerph19053059] [PMID: 35270750]

[25] Emerald, B.S.; Mohsin, S.; D'Souza, C.; John, A.; El-Hasasna, H.; Ojha, S.; Raza, H.; al-Ramadi, B.; Adeghate, E. Diabetes Mellitus alters the immuno-expression of neuronal nitric oxide synthase in the rat pancreas. *Int J Mol Sci,* **2022**, *23*(9), 4974. [http://dx.doi.org/10.3390/ijms23094974] [PMID: 35563364]

[26] Yaribeygi, H.; Sathyapalan, T.; Atkin, S.L.; Sahebkar, A. Molecular mechanisms linking oxidative stress and Diabetes Mellitus. *Oxid Med Cell Longev,* **2020**, *2020*, 1-13. [http://dx.doi.org/10.1155/2020/8609213] [PMID: 32215179]

[27] Anees, L.M.; Abdel-Hamid, G.R.; Elkady, A.A. A nano based

approach to alleviate cisplatin induced nephrotoxicity. *Int J Immunopathol Pharmacol,* **2021**, *35*, 20587384211066441. [http://dx.doi.org/10.1177/20587384211066441] [PMID: 34915755]

[28] Konda, V.R.; Arunachalam, R.; Eerike, M.; Rao K, R.; Radhakrishnan, A.K.; Raghuraman, L.P.; Meti, V.; Devi, S. Nephroprotective effect of ethanolic extract of *Azima tetracantha* root in glycerol induced acute renal failure in Wistar albino rats. *J Tradit Complement Med,* **2016**, *6*(4), 347-354. [http://dx.doi.org/10.1016/j.jtcme.2015.05.001] [PMID: 27774418]

[29] Zhang, S.; Xu, H.; Yu, X.; Wu, Y.; Sui, D. Metformin ameliorates diabetic nephropathy in a rat model of low-dose streptozotocin-induced diabetes. *Exp Ther Med,* **2017**, *14*(1), 383-390. [http://dx.doi.org/10.3892/etm.2017.4475] [PMID: 28672943]

[30] Lu, H.J.; Tzeng, T.F.; Liou, S.S.; Da Lin, S.; Wu, M.C.; Liu, I.M. Ruscogenin ameliorates diabetic nephropathy by its anti-inflammatory and anti-fibrotic effects in streptozotocin-induced diabetic rat. *BMC Complement Altern Med,* **2014**, *14*(1), 110. [http://dx.doi.org/10.1186/1472-6882-14-110] [PMID: 24666993]

[31] Oyenihi, A.B.; Chegou, N.N.; Oguntibeju, O.O.; Masola, B. *Centella asiatica* enhances hepatic antioxidant status and regulates hepatic inflammatory cytokines in type 2 diabetic rats. *Pharm Biol,* **2017**, *55*(1), 1671-1678. [http://dx.doi.org/10.1080/13880209.2017.1318293] [PMID: 28447512]

[32] Adki, K.M.; Kulkarni, Y.A. Biomarkers in diabetic neuropathy. *Arch Physiol Biochem,* **2023**, *129*(2), 460-475. [http://dx.doi.org/10.1080/13813455.2020.1837183] [PMID: 33186087]

[33] Morgenstern, J.; Groener, J.B.; Jende, J.M.E.; Kurz, F.T.; Strom, A.; Göpfert, J.; Kender, Z.; Le Marois, M.; Brune, M.; Kuner, R.; Herzig, S.; Roden, M.; Ziegler, D.; Bendszus, M.; Szendroedi, J.; Nawroth, P.; Kopf, S.; Fleming, T. Neuron-specific biomarkers predict hypo- and hyperalgesia in individuals with diabetic peripheral neuropathy. *Diabetologia,* **2021**, *64*(12), 2843-2855. [http://dx.doi.org/10.1007/s00125-021-05557-6] [PMID: 34480211]

[34] Markova, L.; Umek, N.; Horvat, S.; Hadžić, A.; Kuroda, M.; Pintarič, T.S.; Mrak, V.; Cvetko, E. Neurotoxicity of bupivacaine and liposome bupivacaine after sciatic nerve block in healthy and streptozotocin-induced diabetic mice. *BMC Vet Res,* **2020**, *16*(1), 247. [http://dx.doi.org/10.1186/s12917-020-02459-4] [PMID: 32680505]

[35] Kalinski, A.L.; Yoon, C.; Huffman, L.D.; Duncker, P.C.; Kohen, R.; Passino, R.; Hafner, H.; Johnson, C.; Kawaguchi, R.; Carbajal, K.S.; Jara, J.S.; Hollis, E.; Geschwind, D.H.; Segal, B.M.; Giger, R.J. Analysis of the immune response to sciatic nerve injury identifies efferocytosis as a key mechanism of nerve debridement. *eLife,* **2020**, *9*, e60223. [http://dx.doi.org/10.7554/eLife.60223] [PMID: 33263277]

[36] Yang, J.; Liu, Z. Mechanistic pathogenesis of endothelial dysfunction in diabetic nephropathy and retinopathy. *Front Endocrinol,* **2022**, *13*, 816400. [http://dx.doi.org/10.3389/fendo.2022.816400] [PMID: 35692405]

[37] Gheith, O.; Farouk, N.; Nampoory, N.; Halim, M.A.; Al-Otaibi, T. Diabetic kidney disease: World wide difference of prevalence and risk factors. *J Nephropharmacol,* **2015**, *5*(1), 49-56. [PMID: 28197499]

[38] Prajapati, P.; Kumar, A.; Chaudary, R.; Mangrulkar, S.; Arya, M.; Kushwaha, S. A comprehensive review of essential aspects of molecular pathophysiological mechanisms with emerging interventions for sarcopenia in older people. *Curr Mol Pharmacol,* **2024**, *17*(1), e080323214478. [PMID: 36892022]

[39] Jado, J.C.; Humanes, B.; González-Nicolás, M.Á.; Camaño, S.; Lara, J.M.; López, B.; Cercenado, E.; García-Bordas, J.; Tejedor, A.; Lázaro, A. Nephroprotective effect of cilastatin against gentamicin-induced renal injury *in vitro* and *in vivo* without altering its bactericidal efficiency. *Antioxidants,* **2020**, *9*(9), 821. [http://dx.doi.org/10.3390/antiox9090821] [PMID: 32899204]

[40] Li, J.; Wei, G.H.; Huang, H.; Lan, Y.P.; Liu, B.; Liu, H.; Zhang, W.; Zuo, Y.X. Nerve injury-related autoimmunity activation leads to chronic inflammation and chronic neuropathic pain. *Anesthesiology,* **2013**, *118*(2), 416-429. [http://dx.doi.org/10.1097/ALN.0b013e31827d4b82] [PMID: 23340353]

© 2025 The Author(s). Published by Bentham Science Publisher.

This is an open access article distributed under the terms of the Creative Commons Attribution 4.0 International Public License (CC-BY 4.0), a copy of which is available at: https://creativecommons.org/licenses/by/4.0/legalcode. This license permits unrestricted use, distribution, and reproduction in any medium, provided the original author and source are credited.

DISCLAIMER: The above article has been published, as is, ahead-of-print, to provide early visibility but is not the final version. Major publication processes like copyediting, proofing, typesetting and further review are still to be done and may lead to changes in the final published version, if it is eventually published. All legal disclaimers that apply to the final published article also apply to this ahead-of-print version.